



# FEZ1 Plays Dual Roles in Early HIV-1 Infection by Independently Regulating Capsid Transport and Host Interferon-Stimulated Gene Expression

Viacheslav Malikov,<sup>a</sup>  Mojgan H. Naghavi<sup>a</sup>

<sup>a</sup>Department of Microbiology-Immunology, Northwestern University Feinberg School of Medicine, Chicago, Illinois, USA

**ABSTRACT** Fasciculation and elongation factor zeta 1 (FEZ1), a multifunctional kinesin-1 adaptor, binds human immunodeficiency virus type 1 (HIV-1) capsids and is required for efficient translocation of virus particles to the nucleus to initiate infection. However, we recently found that FEZ1 also acts as a negative regulator of interferon (IFN) production and interferon-stimulated gene (ISG) expression in primary fibroblasts and human immortalized microglial cell line clone 3 (CHME3) microglia, a natural target cell type for HIV-1 infection. This raises the question of whether depleting FEZ1 negatively affects early HIV-1 infection through effects on virus trafficking or IFN induction or both. Here, we address this by comparing the effects of FEZ1 depletion or IFN- $\beta$  treatment on early stages of HIV-1 infection in different cell systems with various IFN- $\beta$  responsiveness. In either CHME3 microglia or HEK293A cells, depletion of FEZ1 reduced the accumulation of fused HIV-1 particles around the nucleus and suppressed infection. In contrast, various doses of IFN- $\beta$  had little to no effect on HIV-1 fusion or the translocation of fused viral particles to the nucleus in either cell type. Moreover, the potency of IFN- $\beta$ 's effects on infection in each cell type reflected the level of induction of MxB, an ISG that blocks subsequent stages of HIV-1 nuclear import. Collectively, our findings demonstrate that loss of FEZ1 function impacts infection through its roles in two independent processes, as a direct regulator of HIV-1 particle transport and as a regulator of ISG expression.

**IMPORTANCE** As a hub protein, fasciculation and elongation factor zeta 1 (FEZ1) interacts with a range of other proteins involved in various biological processes, acting as an adaptor for the microtubule (MT) motor kinesin-1 to mediate outward transport of intracellular cargoes, including viruses. Indeed, incoming HIV-1 capsids bind to FEZ1 to regulate the balance of inward/outward motor activity to ensure net forward movement toward the nucleus to initiate infection. However, we recently showed that FEZ1 depletion also induces interferon (IFN) production and interferon-stimulated gene (ISG) expression. As such, it remains unknown whether modulating FEZ1 activity affects HIV-1 infection through its ability to regulate ISG expression or whether FEZ1 functions directly, or both. Using distinct cell systems that separate the effects of IFN and FEZ1 depletion, here we demonstrate that the kinesin adaptor FEZ1 regulates HIV-1 translocation to the nucleus independently of its effects on IFN production and ISG expression.

**KEYWORDS** FEZ1, HIV-1, early infection, interferon induction, interferon-stimulated genes, motor adaptor, trafficking

Like most viruses, HIV-1 exploits the host microtubule (MT) cytoskeleton to mediate its long-range transport to the nucleus in infected cells. MTs form a highly dynamic network that radiates throughout the cell. These networks mediate the intracellular movement of macromolecular cargoes, including viruses, by the inward/retrograde-directed motor, dynein, and the outward/anterograde-directed kinesin family of motors. However, unlike many viruses that directly bind to MT motors to reach the subcellular site of their replication, HIV-1

**Editor** Frank Kirchhoff, Ulm University Medical Center

**Copyright** © 2023 American Society for Microbiology. All Rights Reserved.

Address correspondence to Mojgan H. Naghavi, mojan.naghavi@northwestern.edu.

The authors declare no conflict of interest.

**Received** 3 April 2023

**Accepted** 5 May 2023

**Published** 23 May 2023

employs more indirect strategies to exploit MT motors. HIV-1 requires MT- and dynein-based trafficking to reach the nucleus, but it does not bind to MT motors directly (1, 2). Instead, fasciculation and elongation factor zeta 1 (FEZ1), a multifunctional kinesin-1 adaptor, binds to incoming HIV-1 capsids to enable the virus to regulate its retrograde motility toward the nucleus (3). Structural analysis further identified FEZ1 as a high-affinity HIV-1 capsid-interacting cellular factor (4). Mechanistically, negatively charged poly-glutamate stretches in FEZ1 bind to a ring of positively charged arginine residues within the central capsid hexamer pore to promote early trafficking of incoming viral cores. HIV-1 also exploits the MT-associated regulatory kinase 2 (MARK2) (5), to phosphorylate FEZ1 at serine 58 (S58), which plays a critical role in controlling kinesin-1-based transport toward the nucleus (3, 6). Although kinesin-1 normally mediates outward cargo movement, capsid-bound FEZ1 enables HIV-1 to control the balance of forward and backward (bi-directional) movement of viral particles and their ultimate net forward movement to the nucleus for efficient infection (3). Soon after the discovery of FEZ1, the dynein adaptor bicaudal D2 (BICD2) was found to act as an HIV-1 capsid-specific adaptor for dynein-mediated motility of incoming viral cores (7, 8). In line with their roles as the respective adaptors for kinesin-1 and dynein, both FEZ1 and BICD2 are required for retrograde transport and uncoating (capsid remodeling or disassembly) of incoming cores during early HIV-1 infection (3, 6–8). As such, binding of HIV-1 capsids to MT motor adaptors is now thought to coordinate cytoplasmic transport and uncoating.

Work from our group and others has shown that modulation of FEZ1 expression also impacts infection by diverse RNA and DNA viruses (9–12). Beyond infection, FEZ1 regulates processes such as neuronal development, and in exploring its broader functionality, we recently found that FEZ1 also regulates beta interferon (IFN- $\beta$ ) production and induction of interferon-stimulated genes (ISGs) in a stimulator of interferon genes (STING)-independent manner (13). This function of FEZ1 also requires phosphorylation of S58 in its kinesin regulatory domain, which controls FEZ1 binding to and relocalization of heat shock protein 8 (HSPA8), which in turn influences DNA-dependent protein kinase (DNA-PK) and STING-independent IFN response pathways (13). As such, it remains unclear whether loss of FEZ1 functionality negatively affects early HIV-1 infection through effects on virus trafficking or induction of IFN- $\beta$  and ISG expression or both. To address this, here we investigated the effects of IFN and FEZ1 depletion in distinct cell systems that separate these two processes. Our findings demonstrate that the kinesin adaptor FEZ1 regulates HIV-1 translocation to the nucleus independently of its effects on IFN- $\beta$  production and ISG expression.

## RESULTS

**FEZ1 and IFN- $\beta$  affect distinct stages of HIV-1 infection in CHME3 cells.** Given that depletion of endogenous FEZ1 increases IFN- $\beta$  production and ISG expression in human immortalized microglial cell line clone 3 (CHME3) cells (13), we first tested how IFN- $\beta$  treatment affected early HIV-1 infection in these cells. Treatment with low doses of IFN- $\beta$  increased the expression of several ISGs, namely, MxB, ISG56, and interferon-induced transmembrane 1 (IFITM1), in a manner comparable with that of small interfering RNA (siRNA)-mediated depletion of FEZ1, in line with loss of FEZ1 inducing moderate levels of IFN- $\beta$  production (13) (Fig. 1A). In contrast, higher levels of IFN- $\beta$  resulted in a potent induction of ISGs. Using HIV-1 luciferase reporter viruses pseudotyped with wild-type (WT) envelope (HIV-1-WT-Luc), we showed that similar to CHME3 cells depleted of FEZ1 (3; Fig. 1B), these IFN- $\beta$  treatments resulted in a corresponding decrease in HIV-1 infection (Fig. 1C and D). To better understand how IFN- $\beta$  treatment affected early infection, these cells were infected with a double-labeled HIV-1 (S15-tomato labeling viral membrane and green fluorescent protein (GFP)-Vpr labeling viral core) carrying WT envelope (HIV-1-DL-WT), followed by analysis of samples fixed and stained for p24 by confocal microscopy. The maximum p24 fluorescence intensity associated with each virus particle that had successfully fused and entered the cytoplasm was then measured. Fused particles shed the S15-tomato-labeled viral membrane (S15-tomato<sup>-</sup>/GFP-Vpr<sup>+</sup>) and appeared green, while unfused particles that might have been nonproductively endocytosed retained both labels (S15-tomato<sup>+</sup>/GFP-Vpr<sup>+</sup>) and appeared yellow (Fig. 2A). Importantly, these virus preparations were >95% double-labeled. The data

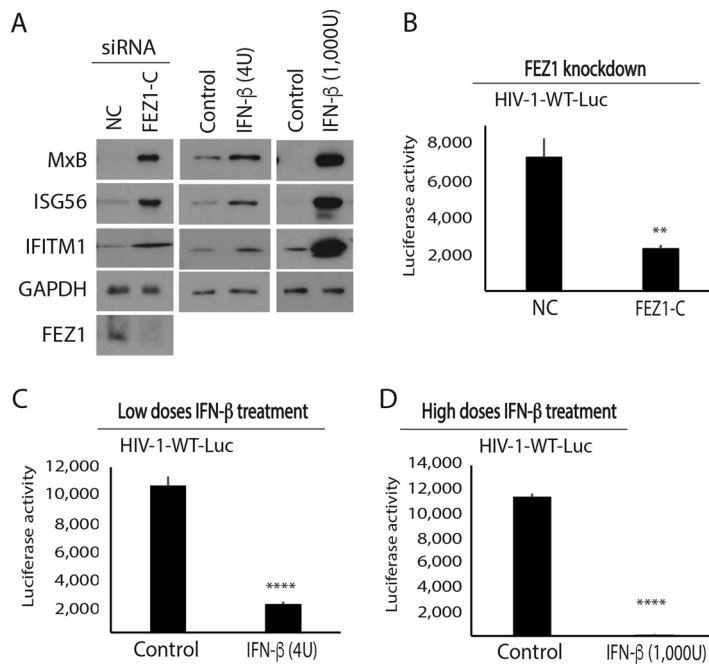


**FIG 1** FEZ1 depletion or IFN- $\beta$  treatment reduces early HIV-1 infection in CHME3 cells. (A) Western blot (WB) analysis showing ISG (MxB, ISG56, and IFITM1) levels in CHME3 cells either treated with the negative control (NC) or FEZ1-specific siRNAs (FEZ1-C) or with various concentrations of IFN- $\beta$  (low, 4 U; high, 1,000 U, respectively). (B to D) CHME3 cells treated with either NC or FEZ1-C siRNAs (B) or with low (C) or high (D) IFN- $\beta$  concentrations were infected with HIV-1 carrying a luciferase reporter and pseudotyped with WT envelope (HIV-1-WT-Luc) followed by measurements of luciferase activity. Data are shown as the mean  $\pm$  SD. Statistical significance was calculated using a *t* test. \*\*,  $P \leq 0.01$ ; \*\*\*\*,  $P \leq 0.0001$ . Results are representative of 3 independent biological repeats except in panel B, where the results are representative of 2 experimental replicates.

revealed that similar to FEZ1 depletion (3; Fig. 2B), IFN- $\beta$  treatments did not affect the number of fused (green) viral particles compared with controls within an hour postinfection (hpi) into the cytosol (Fig. 2C and D). Measuring the distance of the fused HIV-1 particles from the nucleus revealed that there was a significant reduction in the proportion of fused particles that reached within 2  $\mu$ m of the nucleus in FEZ1-depleted cells compared with control siRNA-treated CHME3 cells (Fig. 2E), in line with our previous report using vesicular stomatitis virus (VSV) pseudotyped double-labeled HIV-1 (HIV-1-DL-VSV) in primary human fibroblasts (3). This is in line with our broader understanding that FEZ1 is required for the trafficking of incoming viral cores to the nucleus (3, 4). In contrast, the number of fused viral particles reaching the vicinity of the nucleus was unchanged in IFN-treated CHME3 cells, with the exception of a modest reduction at later time points in cells treated with the highest concentration of IFN- $\beta$  (Fig. 2F–G). These combined data demonstrate that, unlike FEZ1, IFN and its associated induction of ISG expression do not affect migration of incoming HIV-1 cores toward the nucleus but, instead, block HIV-1 infection at a later stage after translocation to the nucleus. This is in line with findings that MxB acts as a key effector of the antiviral activity of IFN against HIV-1 and that it blocks HIV-1 nuclear import (14–16).

**Effects of IFN- $\beta$  and FEZ1 depletion on infection in HEK293A cells further support the specific role of FEZ1 in HIV-1 transport to the nucleus.** Given that HEK293 cells are known to be defective in several IFN and antiviral response pathways, we next tested how IFN- $\beta$  treatment affected early HIV-1 infection in these cells. In doing so, we found that while treatment of HEK293A cells with either high or low doses of IFN- $\beta$  induced ISG56 and IFITM1, only very low levels of MxB induction were detected at the highest doses of IFN- $\beta$  tested (Fig. 3A). Further, in line with the notion that MxB is a major effector of IFN- $\beta$ 's activity against HIV-1, infecting these cells using HIV-1-VSV-Luc reporter virus, we further found that low doses of IFN- $\beta$  had no effect on HIV-1 infection (Fig. 3B), while higher doses reduced infection by approximately 2-fold (Fig. 3C). The same results were obtained using higher input doses of the HIV-1VSV-Luc reporter virus (Fig. 3D and E, respectively). To

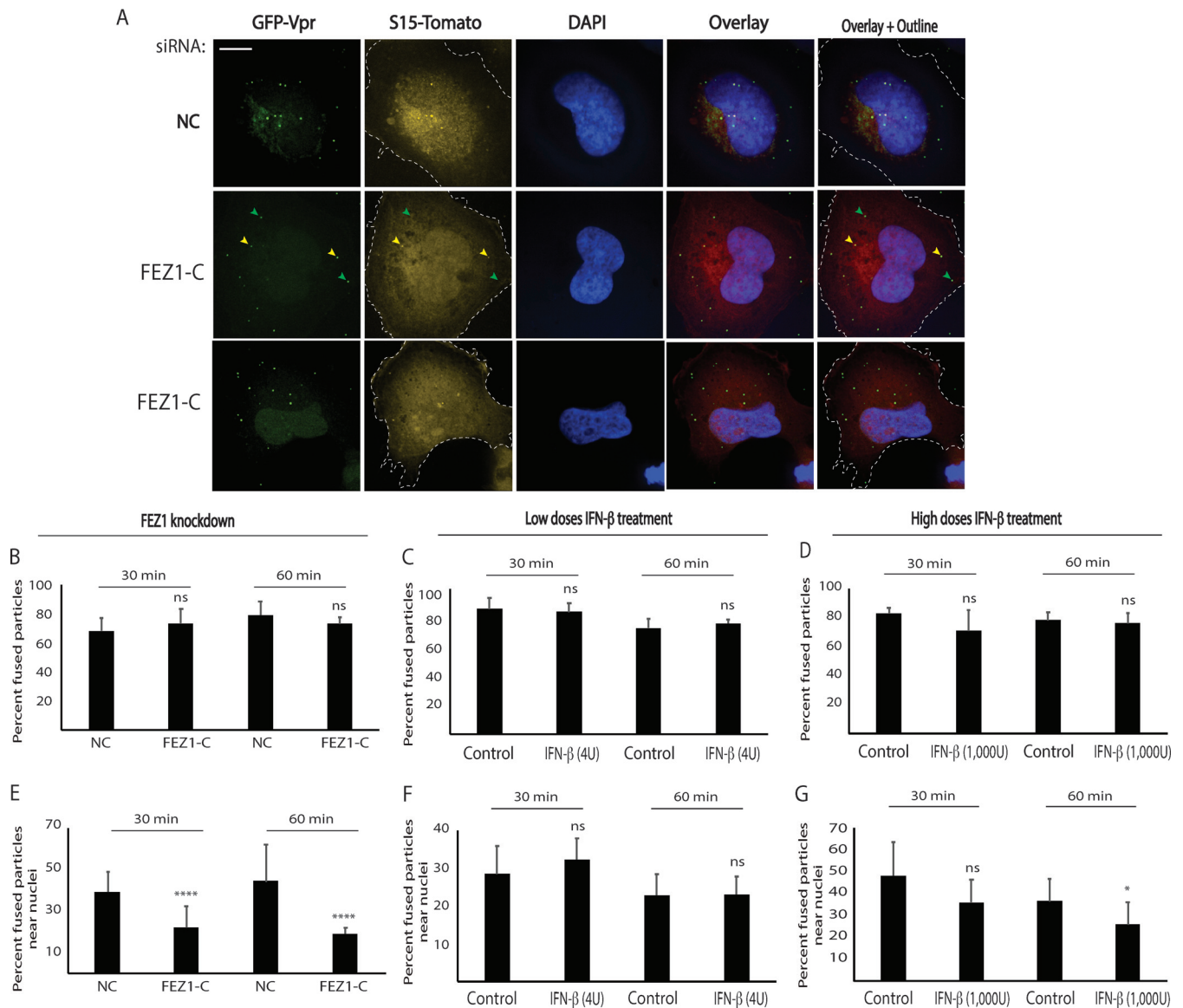


**FIG 2** FEZ1, but not IFN- $\beta$ , regulates HIV-1 translocation to the nucleus in CHME3 cells. (A) Representative images showing that depletion of FEZ1 affects nuclear translocation of HIV-1 particles that have productively fused into the cytoplasm. CHME3 cells were treated with the negative control (NC) or FEZ1-specific siRNAs (FEZ1-C). Then, 48 h posttransfection cells were infected with double-labeled HIV-1 (S15-tomato/GFP-Vpr) carrying a WT envelope (HIV-1-DL-WT); 60 min postinfection cells were fixed and GFP and tomato signals were acquired using a spinning-disc confocal microscope. The cell periphery is outlined. (Middle row) Arrows highlight examples of fused (green, S15-tomato<sup>-</sup>/GFP-Vpr<sup>+</sup>) and unfused (yellow, S15-tomato<sup>+</sup>/GFP-Vpr<sup>+</sup>) viral particles. (B to G) CHME3 cells treated with either NC or FEZ1-C siRNAs (B and E) or with various concentrations of IFN- $\beta$  (low, 4 U; high, 1000 U, respectively) (C and F and D and G, respectively) as in Fig. 1 were infected with HIV-1-DL-WT followed by measurements of the number of fused particles in cells fixed at the indicated time postinfection as in panel A. The percentage of fused HIV-1-DL-WT into the cytosol (B to D) or their accumulation within 2  $\mu$ m of the nucleus (E to G) is shown. Data in panels B to G represent the mean of  $\geq 800$  virus particles analyzed in  $\geq 55$  fields of view ( $\geq 56$  cells) for each condition. Data are shown as the mean  $\pm$  SD. Statistical significance was calculated using a *t* test. \*,  $P \leq 0.05$ ; \*\*\*\*,  $P \leq 0.0001$ ; ns, not significant. Results are representative of 3 independent biological repeats except in panels B and E, which are representative of 2 experimental replicates.

investigate whether ISG induction in HEK293A cells upon high-dose IFN- $\beta$  treatment affected nuclear translocation of HIV-1, these cells were infected with HIV-1-DL-VSV. Analysis of fixed samples showed that HIV-1 fusion (Fig. 3F and G) or accumulation of fused (green) virus particles near the nucleus (Fig. 3H and I) were not affected in IFN- $\beta$ -treated HEK293A cells. Comparing these results with the potent induction of MxB expression and suppression of infection in IFN- $\beta$ -treated CHME3 cells, these combined data support the idea that MxB is the primary effector or determinant of IFN- $\beta$ 's effects on early HIV-1 infection in these two cell systems (14–16). Moreover, because of the potency of MxB's antiviral effects in CHME3 cells, these findings also highlighted the potential utility of HEK293A cells in investigating

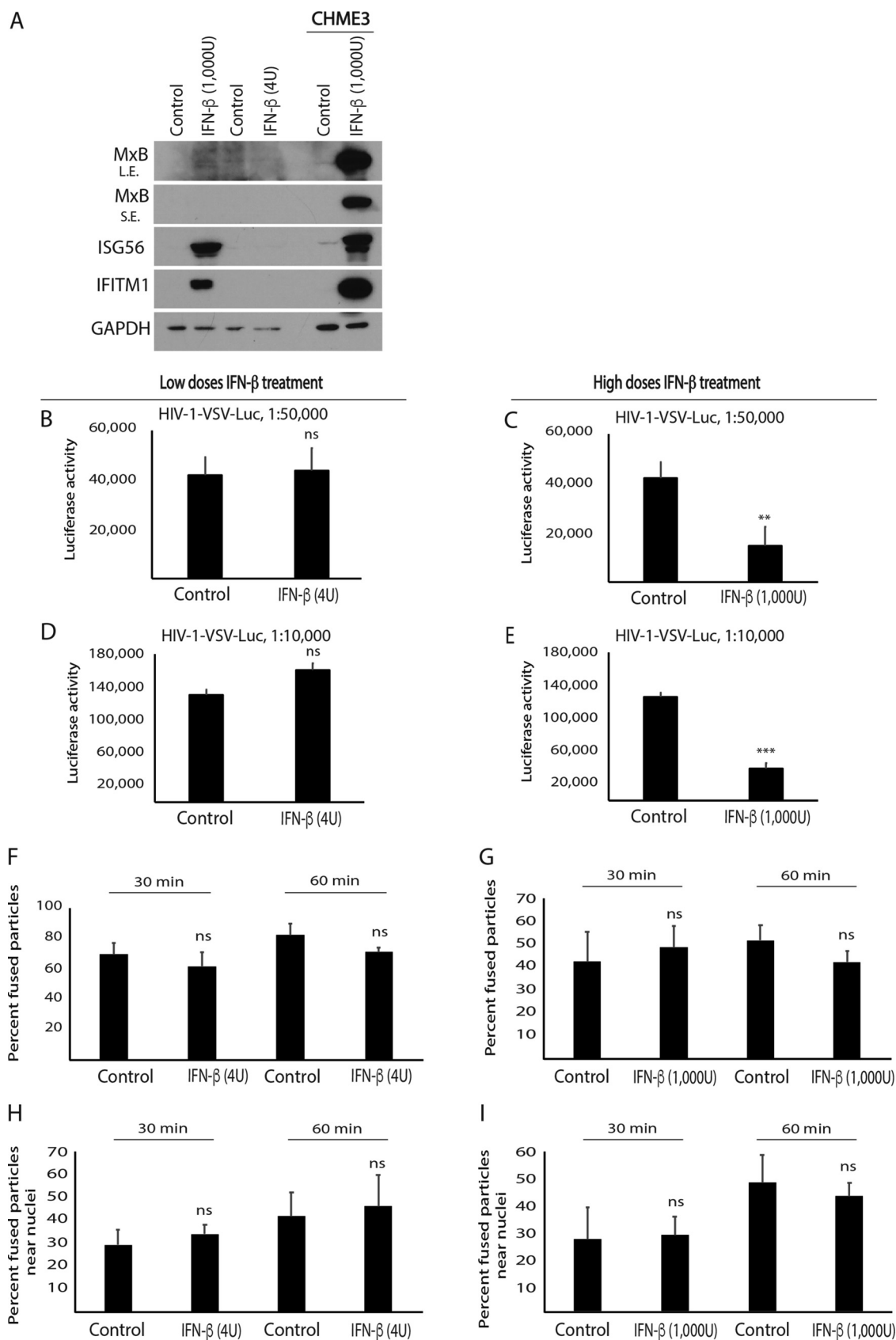


**FIG 3** IFN- $\beta$  does not affect HIV-1 translocation to the nucleus in HEK293A cells. (A) WB analysis showing ISG (MxB, ISG56, and IFITM1) levels in HEK293A cells treated with various concentrations of IFN- $\beta$  (low, 4 U; high, 1,000 U). Control or IFN- $\beta$  treated CHME3 (Continued on next page)



the effect of FEZ1 on trafficking and early infection with fewer complications from IFN and ISG responses.

The findings described above suggest that the ability of FEZ1 to regulate ISG expression is likely independent of its effect on virus transport. To independently test this, we determined the effects of FEZ1 depletion on ISG expression and early HIV-1 infection in HEK293A cells. Unlike in CHME3 cells (Fig. 1A), depletion of FEZ1 using either of two independent siRNAs did not increase ISG expression in HEK293A cells (Fig. 4A). To test whether FEZ1 depletion affected nuclear translocation of viral particles, siRNA-treated HEK293A cells were infected with HIV-1-DL-VSV followed by analysis of fixed samples. In doing so, we found that despite a lack of ISG induction in HEK293A cells, FEZ1 resulted in a significant reduction in the accumulation of fused virus particles near the nucleus as early as 30 min postinfection without affecting their fusion into the cytosol (Fig. 4B and C). By infecting these cells with various amounts of HIV-1-Luc reporter pseudotyped with VSV envelope (HIV-1-VSV-Luc), we further showed that the defect in HIV-1 nuclear translocation resulted in a corresponding decrease in infection (Fig. 4D and E). Combined, these findings demonstrate that FEZ1 regulates HIV-1 translocation to the nucleus independently of its effects on IFN production and ISG expression.

## DISCUSSION

FEZ1 plays a complex role in both host interferon response pathways and viral infection. In the case of HIV-1, FEZ1 binds directly to incoming HIV-1 capsids and regulates their retrograde motility for efficient infection (3, 4, 6), yet more recently, we discovered that FEZ1 also functions as a negative regulator of host IFN production and ISG expression (13). As such, this raised the simple but important question as to whether previously reported effects of FEZ1 depletion on early HIV-1 arise due to induction of IFN- $\beta$  and ISG expression rather than its role as a viral transport protein.

Here, we show that FEZ1 regulates early transport of incoming HIV-1 cores toward the nucleus and that this specific process in infection is not affected by IFN- $\beta$  or ISG induction. However, our data also highlight the complexity of understanding FEZ1's overall impact on infection in cell types that retain intact interferon response pathways, due to the impact of ISGs on subsequent steps in HIV-1 infection. While we find that IFN- $\beta$  treatment of CHME3 cells did not impact the fusion or cytoplasmic translocation of fused virus particles toward the nucleus, IFN- $\beta$  still potently suppressed early infection in these cells. These findings are in line with a growing number of studies from independent groups suggesting that ISG responses primarily block early HIV-1 infection at stages at or after nuclear entry steps (17–22). This includes MxB, which blocks nuclear import and is thought to be a key effector of IFN's inhibitory effects on HIV-1 infection (14–16). As a result, the contribution of any defects in virus trafficking to the overall magnitude of defects in HIV-1 infection during FEZ1 depletion are likely to be confounded by the potency of the block to subsequent nuclear import steps that are imposed by ISGs. While these two distinct functions of FEZ1 are challenging to uncouple experimentally, because they are regulated in the same way, our findings here using distinct cell systems now demonstrate that HIV-1 does indeed exploit FEZ1 for capsid transport while the host cell uses FEZ1 to control the antiviral state.

Further supporting this notion, we reveal the utility of HEK293A cells as a means to avoid the complexity of contributions from IFN and ISG responses. Interestingly, IFN- $\beta$  is far less potent in terms of its antiviral activity in these cells, and this correlates with little to no induction of MxB, despite induction of other ISGs tested. More importantly, we further show that

### FIG 3 Legend (Continued)

cells were included as the positive control for ISG induction. L.E., long exposure; S.E., short exposure. (B to I) HEK293A cells treated with low (B and D) or high (C and E) IFN- $\beta$  concentrations were infected either with HIV-1 carrying a luciferase reporter and pseudotyped with VSV envelope (HIV-1-VSV-luc) at two different dilutions as indicated followed by measurements of luciferase activity (B–E) or with double-labeled HIV-1 (S15-tomato/GFP-Vpr) carrying a VSV envelope (HIV-1-DL-VSV) followed by measurements of the number of fused particles (S15-tomato<sup>-</sup>/GFP-Vpr<sup>+</sup>) in cells fixed at the indicated time postinfection (F–I). The percentage of double-labeled HIV-1-DL-VSV fused into the cytosol (F and G) or their accumulation within 2  $\mu$ m of the nucleus (H and I) is shown. Data in panels F to I represent the mean of  $\geq 730$  virus particles analyzed in  $\geq 55$  fields of view ( $\geq 60$  cells) for each condition. Data are shown as mean  $\pm$  SD. Statistical significance was calculated using a *t* test (B to I). \*\*,  $P \leq 0.01$ ; \*\*\*,  $P \leq 0.001$ ; ns, not significant. Results in panels A to E are representative of 3 and in panels F to I of 2 independent biological repeats.

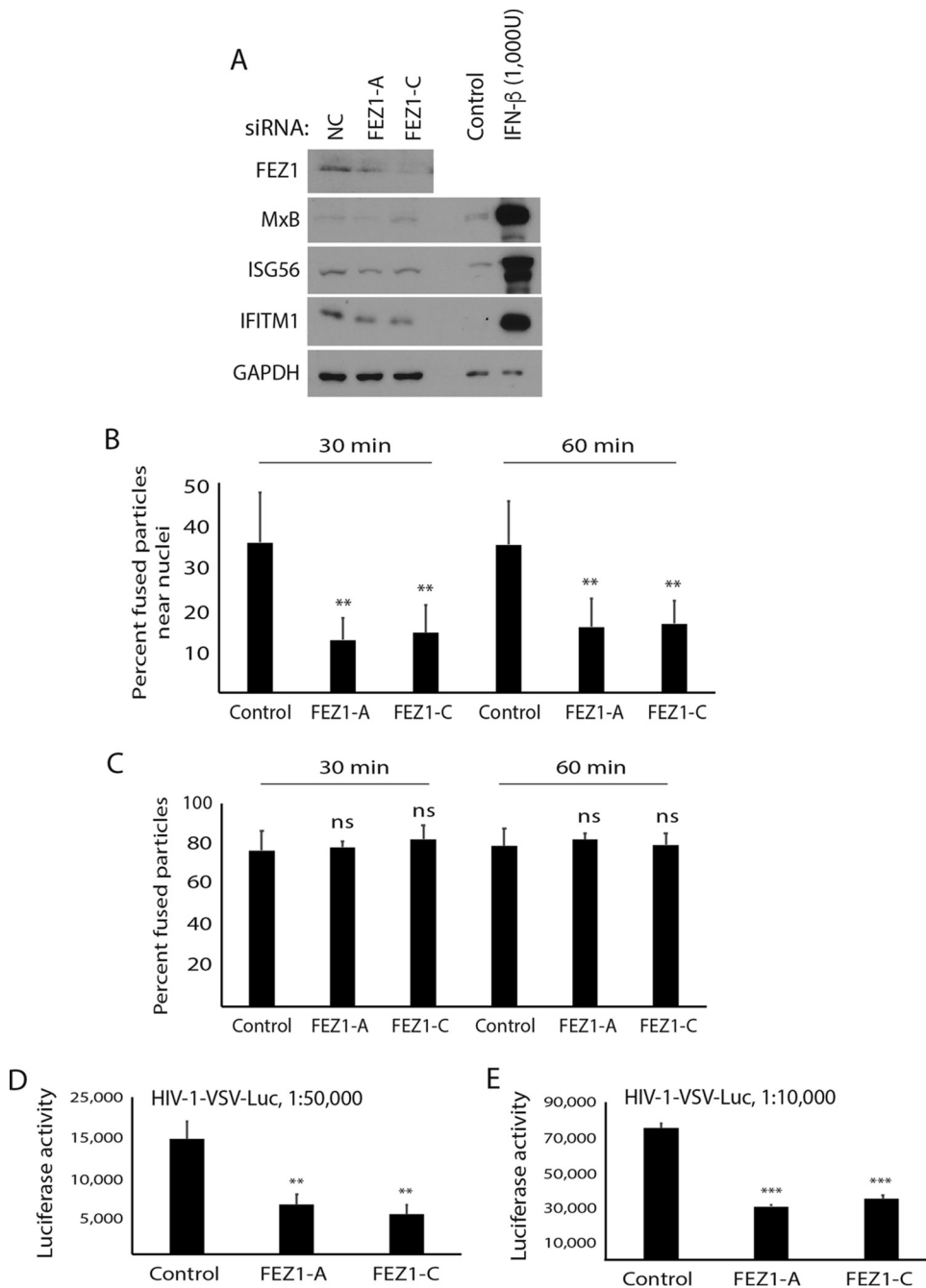


**FIG 4** FEZ1 depletion does not induce ISGs but suppresses early HIV-1 infection in HEK293A cells. (A) WB analysis showing ISG (MxB, ISG56, IFITM1) levels in HEK293A cells treated with either the negative control (NC) or two independent FEZ1-specific siRNAs (FEZ1-A and FEZ1-C). Control or IFN-β-treated CHME3 cells were included as the positive control for ISG induction. (B and C) NC or FEZ1 siRNA-treated HEK293A cells were infected with double-labeled HIV-1 (S15-tomato/GFP-Vpr) carrying a VSV envelope (HIV-1-DL-VSV) followed by measurements of the number of fused particles (S15-tomato<sup>+</sup>/GFP-Vpr<sup>+</sup>) in cells fixed at the indicated times postinfection. The percentage of accumulation of fused HIV-1-DL-VSV within 2 μm of the nucleus (B) or their fusion into the cytosol (C) is shown. Data in panels B and C represent the mean of ≥750 virus particles analyzed in ≥50 fields of view (≥55 cells) for each condition. (D and E) NC or FEZ1 siRNA-treated HEK293A cells were infected with HIV-1 carrying a luciferase reporter and pseudotyped with VSV envelope (HIV-1-VSV-Luc) at two different dilutions as indicated followed by measurements of luciferase activity. Data are shown as the mean ± SD. Statistical significance was calculated using ANOVA with Tukey's *post hoc* test (B to E). \*\*, *P* ≤ 0.01; \*\*\*, *P* ≤ 0.001; ns, not significant. Results in panels A to C and E are representative of 3 and in panel D of 2 independent biological repeats.

FEZ1 depletion does not induce ISGs in HEK293A cells but significantly reduces the number of productively fused virus particles reaching the vicinity of the nucleus. Combined, our findings demonstrate that the kinesin adaptor FEZ1 regulates HIV-1 translocation to the nucleus independently of its effects on IFN production and ISG expression. Indeed, the dynein adaptor for HIV-1, BICD2, also regulates both HIV-1 particle motility and host responses to infection (7). Our findings add new insights into how motor adaptors that are exploited by HIV-1 to regulate its trafficking also function independently to control host responses, perhaps sensing when pathogens coopt their activity.

## MATERIALS AND METHODS

**Cell lines and IFN- $\beta$  treatments.** Human immortalized microglial cell line clone 3 (CHME3) was described previously (23), and HEK293A cells were obtained from ATCC. Cells were cultured in Dulbecco's modified Eagle's medium (DMEM; Fisher Scientific) containing 10% Nu-Serum culture supplement (Corning), 2 mM L-glutamine, 100 U/mL penicillin, 100  $\mu$ g/mL streptomycin, and 1 mM sodium pyruvate for CHME3 cells. For IFN- $\beta$  treatments, culture medium was replaced with fresh medium containing human recombinant IFN- $\beta$  (EMD Millipore) at the indicated concentrations for 24 h.

**Reporter viruses, infections, and luciferase reading.** Stocks of HIV-1-Luc-VSV and HIV-1-Luc-WT viruses were prepared as described previously (6). Cells pretreated with IFN- $\beta$  for 24 h or transfected with siRNAs for 48 h, were incubated in the presence of 8  $\mu$ g/mL polybrene with HIV-1-Luc-VSV for 8 h or with HIV-1-Luc-WT overnight followed by replacement of the culture medium with fresh medium. Luciferase activity was measured 48 h postinfection using the luciferase assay system (Promega).

**Knockdowns.** Expression of FEZ1 was transiently suppressed by using RNA interference (RNAi) as previously described (13). Briefly, CHME3 and HEK293A cells were plated in 12-well plates in normal growth medium omitting antibiotics at 80,000 cells/well. The next day they were transfected with 100 pM of NC1 (ID no. AM4635), FEZ1-A (ID no. 15759), and FEZ1-C (ID no. 45101) siRNAs for HEK293A or with NC1 and FEZ1-C for CHME3 cells. After 24 h cells were split onto coverslips in 24-well plates for HIV-1 trafficking analysis. After 48 h cells were lysed with Laemmli loading buffer to determine the level of knockdown or were infected with corresponding virus stock to assess infection efficacy.

**Western blotting.** Proteins in samples were separated in 10% SDS-PAGE and transferred to nitrocellulose membranes as described (13). Membranes were blocked in 3% nonfat milk in Tris-buffered saline with Tween 20 (TBS-T) for 1 h, washed, and incubated with primary antibodies overnight at +4°C. The primary antibodies anti-FEZ1 (no. 42480), anti-MxB (no. 43924), and anti-ISG56 (no. 14769) from Cell Signaling, anti-IFITM1 (11727-3-AP) from Proteintech, and anti-GAPDH (sc-25778) from Santa Cruz were diluted at 1:1,000 in 3% bovine serum albumin (BSA) in TBS-T. Appropriate secondary antibodies conjugated with horseradish peroxidase (HRP) were bound during 1 h of incubation at room temperature. Protein bands were detected using Pierce ECL or Femto high-sensitivity Western blotting substrates (Thermo Fisher Scientific).

**Microscopy and HIV-1 trafficking analysis.** In order to evaluate HIV-1 trafficking, CHME3 and HEK293A cells were treated with IFN- $\beta$  or transfected with siRNAs and plated onto gelatin-coated coverslips. Then, CHME3 cells were infected with double-labeled HIV-1-GFP-Vpr-WTenv-S15-tomato and HEK293A with double-labeled HIV-1-GFP-Vpr-VSVenv-S15-tomato using spinoculation as previously described (3). Incorporation of S15-tomato in the virus particles labeled with GFP-Vpr was greater than 95%. Both stocks were diluted at 1:50 with CO<sub>2</sub>-independent medium supplemented with 5% Nu-Serum, 2 mM L-glutamine, and 8  $\mu$ g/mL polybrene. Media on the cells were substituted with diluted virus stocks, and plates were centrifuged for 30 min at 1,200  $\times$  g in a centrifuge prechilled at 13°C. Infections were started with 2 brief washes of growth medium with 8  $\mu$ g/mL polybrene prewarmed at 37°C and were stopped at the specified time intervals by fixing cells with 3.7% paraformaldehyde (PFA) in phosphate-buffered saline (PBS) for 15 min. Fixed cells were permeabilized for 30 min with 0.1% saponin in PBS containing 10% donkey normal serum, rinsed twice, and washed once with PBS for 5 min. Cell nuclei were stained with 20  $\mu$ g/mL Hoechst 33342 for 20 min. Coverslips were washed thrice with PBS for 5 min, rinsed with water, partially dried, and fixed onto glass slides with FluorSave reagent (Calbiochem). Confocal images were acquired using a Leica DMI 6000B motorized microscope equipped with a Hamamatsu Imagem X2 electron multiplying charge coupled device (EMCCD) camera and run by Metamorph imaging software. Productively fused virus particles were S15-tomato negative and GFP-Vpr positive. The numbers of fused particles near nuclei and in the cytoplasm were counted in Metamorph imaging software.

**Statistical analyses.** Statistical significance was tested with Student's *t* test for two groups and with one-way analysis of variance (ANOVA) with Turkey's *post hoc* test when more than two groups were compared. Data are represented as means  $\pm$  standard deviations (SD). ANOVA with posttest was used when more than two groups were compared. Statistical significance is shown as follows: \*,  $P \leq 0.05$ ; \*\*,  $P \leq 0.01$ ; \*\*\*,  $P \leq 0.001$ ; and \*\*\*\*,  $P \leq 0.0001$ , respectively.

## ACKNOWLEDGMENTS

pNL4-3.luc.R<sup>-</sup>E<sup>-</sup> was obtained through the NIH AIDS Reagent Program, Division of AIDS, NIAID, NIH. This work was supported by NIH grant R01 AI150559 to M.H.N.

We declare no conflict of interest.



## REFERENCES

- McDonald D, Vodicka MA, Lucero G, Svitkina TM, Borisy GG, Emerman M, Hope TJ. 2002. Visualization of the intracellular behavior of HIV in living cells. *J Cell Biol* 159:441–452. <https://doi.org/10.1083/jcb.200203150>.
- Arhel N, Genovesio A, Kim KA, Miko S, Perret E, Olivo-Marin JC, Shorte S, Charneau P. 2006. Quantitative four-dimensional tracking of cytoplasmic and nuclear HIV-1 complexes. *Nat Methods* 3:817–824. <https://doi.org/10.1038/nmeth928>.
- Malikov V, da Silva ES, Jovasevic V, Bennett G, de Souza Aranha Vieira DA, Schulte B, Diaz-Griffero F, Walsh D, Naghavi MH. 2015. HIV-1 capsids bind and exploit the kinesin-1 adaptor FEZ1 for inward movement to the nucleus. *Nat Commun* 6:6660. <https://doi.org/10.1038/ncomms7660>.
- Huang PT, Summers BJ, Xu C, Perilla JR, Malikov V, Naghavi MH, Xiong Y. 2019. FEZ1 is recruited to a conserved cofactor site on capsid to promote HIV-1 trafficking. *Cell Rep* 28:2373–2385.e7. <https://doi.org/10.1016/j.celrep.2019.07.079>.
- Chua JJ, Butkevich E, Worsceck JM, Kittelmann M, Gronborg M, Behrmann E, Stelzl U, Pavlos NJ, Lalowski MM, Eimer S, Wanker EE, Kloppenstein DR, Jahn R. 2012. Phosphorylation-regulated axonal dependent transport of syntaxin 1 is mediated by a Kinesin-1 adaptor. *Proc Natl Acad Sci U S A* 109:5862–5867. <https://doi.org/10.1073/pnas.1113819109>.
- Malikov V, Naghavi MH. 2017. Localized phosphorylation of a kinesin-1 adaptor by a capsid-associated kinase regulates HIV-1 motility and uncoating. *Cell Rep* 20:2792–2799. <https://doi.org/10.1016/j.celrep.2017.08.076>.
- Dharan A, Opp S, Abdel-Rahim O, Keceli SK, Imam S, Diaz-Griffero F, Campbell EM. 2017. Bicaudal D2 facilitates the cytoplasmic trafficking and nuclear import of HIV-1 genomes during infection. *Proc Natl Acad Sci U S A* 114:E10707–E10716. <https://doi.org/10.1073/pnas.1712033114>.
- Carnes SK, Zhou J, Aiken C. 2018. HIV-1 engages a dynein-dynactin-BICD2 complex for infection and transport to the nucleus. *J Virol* 92:e00358-18. <https://doi.org/10.1128/JVI.00358-18>.
- Gao G, Goff SP. 1999. Somatic cell mutants resistant to retrovirus replication: intracellular blocks during the early stages of infection. *Mol Biol Cell* 10:1705–1717. <https://doi.org/10.1091/mbc.10.6.1705>.
- Naghavi MH, Hatzioannou T, Gao G, Goff SP. 2005. Overexpression of fasciculation and elongation protein zeta-1 (FEZ1) induces a post-entry block to retroviruses in cultured cells. *Genes Dev* 19:1105–1115. <https://doi.org/10.1101/gad.1290005>.
- Suzuki T, Okada Y, Semba S, Orba Y, Yamanouchi S, Endo S, Tanaka S, Fujita T, Kuroda S, Nagashima K, Sawa H. 2005. Identification of FEZ1 as a protein that interacts with JC virus agnoprotein and microtubules: role of agnoprotein-induced dissociation of FEZ1 from microtubules in viral propagation. *J Biol Chem* 280:24948–24956. <https://doi.org/10.1074/jbc.M411499200>.
- Haedicke J, Brown C, Naghavi MH. 2009. The brain-specific factor FEZ1 is a determinant of neuronal susceptibility to HIV-1 infection. *Proc Natl Acad Sci U S A* 106:14040–14045. <https://doi.org/10.1073/pnas.0900502106>.
- Malikov V, Meade N, Simons LM, Hultquist JF, Naghavi MH. 2022. FEZ1 phosphorylation regulates HSPA8 localization and interferon-stimulated gene expression. *Cell Rep* 38:110396. <https://doi.org/10.1016/j.celrep.2022.110396>.
- Goujon C, Moncorge O, Bauby H, Doyle T, Ward CC, Schaller T, Hue S, Barclay WS, Schulz R, Malim MH. 2013. Human MX2 is an interferon-induced post-entry inhibitor of HIV-1 infection. *Nature* 502:559–562. <https://doi.org/10.1038/nature12542>.
- Kane M, Yadav SS, Bitzegeio J, Kutluay SB, Zang T, Wilson SJ, Schoggins JW, Rice CM, Yamashita M, Hatzioannou T, Bieniasz PD. 2013. MX2 is an interferon-induced inhibitor of HIV-1 infection. *Nature* 502:563–566. <https://doi.org/10.1038/nature12653>.
- Liu Z, Pan Q, Ding S, Qian J, Xu F, Zhou J, Cen S, Guo F, Liang C. 2013. The interferon-inducible MxB protein inhibits HIV-1 infection. *Cell Host Microbe* 14:398–410. <https://doi.org/10.1016/j.chom.2013.08.015>.
- Chintala K, Mohareer K, Banerjee S. 2021. Dodging the host interferon-stimulated gene mediated innate immunity by HIV-1: a brief update on intrinsic mechanisms and counter-mechanisms. *Front Immunol* 12:716927. <https://doi.org/10.3389/fimmu.2021.716927>.
- Sertznig H, Roesmann F, Wilhelm A, Heining D, Bleekmann B, Elsner C, Santiago M, Schuhenn J, Karakoese Z, Benatzky Y, Snodgrass R, Esser S, Sutter K, Dittmer U, Widera M. 2022. SRSF1 acts as an IFN-I-regulated cellular dependency factor decisively affecting HIV-1 post-integration steps. *Front Immunol* 13:935800. <https://doi.org/10.3389/fimmu.2022.935800>.
- Buckmaster MV, Goff SP. 2022. Riplet binds the zinc finger antiviral protein (ZAP) and augments ZAP-mediated restriction of HIV-1. *J Virol* 96:e0052622. <https://doi.org/10.1128/jvi.00526-22>.
- Olson RM, Gornalusse G, Whitmore LS, Newhouse D, Tisoncik-Go J, Smith E, Ochsenbauer C, Hladik F, Gale M, Jr. 2022. Innate immune regulation in HIV latency models. *Retrovirology* 19:15. <https://doi.org/10.1186/s12977-022-00599-z>.
- Taura M, Frank JA, Takahashi T, Kong Y, Kudo E, Song E, Tokuyama M, Iwasaki A. 2022. APOBEC3A regulates transcription from interferon-stimulated response elements. *Proc Natl Acad Sci U S A* 119:e2011665119. <https://doi.org/10.1073/pnas.2011665119>.
- Jurczyszak D, Manganaro L, Buta S, Gruber C, Martin-Fernandez M, Taft J, Patel RS, Cipolla M, Alshammery H, Mulder LCF, Sachidanandam R, Bogunovic D, Simon V. 2022. ISG15 deficiency restricts HIV-1 infection. *PLoS Pathog* 18:e1010405. <https://doi.org/10.1371/journal.ppat.1010405>.
- Janabi N, Peudenier S, Heron B, Ng KH, Tardieu M. 1995. Establishment of human microglial cell lines after transfection of primary cultures of embryonic microglial cells with the SV40 large T antigen. *Neurosci Lett* 195:105–108. [https://doi.org/10.1016/0304-3940\(94\)11792-h](https://doi.org/10.1016/0304-3940(94)11792-h).